



HAL
open science

Cavity ring down spectroscopy of water vapor near 750 nm: a test of the HITRAN2020 and W2020 line lists

S. Vasilchenko, S.N. Mikhailenko, A. Campargue

► **To cite this version:**

S. Vasilchenko, S.N. Mikhailenko, A. Campargue. Cavity ring down spectroscopy of water vapor near 750 nm: a test of the HITRAN2020 and W2020 line lists. *Molecular Physics*, 2022, 120 (15-16), 10.1080/00268976.2022.2051762 . hal-03865608

HAL Id: hal-03865608

<https://hal.science/hal-03865608>

Submitted on 22 Nov 2022

HAL is a multi-disciplinary open access archive for the deposit and dissemination of scientific research documents, whether they are published or not. The documents may come from teaching and research institutions in France or abroad, or from public or private research centers.

L'archive ouverte pluridisciplinaire **HAL**, est destinée au dépôt et à la diffusion de documents scientifiques de niveau recherche, publiés ou non, émanant des établissements d'enseignement et de recherche français ou étrangers, des laboratoires publics ou privés.

Cavity ring down spectroscopy of water vapor near 750 nm: a test of the HITRAN2020 and W2020 line lists

S. Vasilchenko ^a, S.N. Mikhailenko ^{a,b}, A. Campargue ^{c*},

^a V.E. Zuev Institute of Atmospheric Optics, SB, Russian Academy of Science, 1, Academician Zuev square, 634055 Tomsk, Russia

^b Climate and Environmental Physics Laboratory, Ural Federal University, 19, Mira av., 620002 Yekaterinburg, Russia

^c Univ. Grenoble Alpes, CNRS, LIPhy, 38000 Grenoble, France

Key words: water vapor; H₂O; absorption spectroscopy; rovibrational energy level; HITRAN

Number of Pages: 28
Number of Figures: 9
Number of Tables: 2

Corresponding author

E-mail address: Alain.Campargue@univ-grenoble-alpes.fr

Tel.: 33 4 76 51 43 19 Fax. 33 4 76 63 54 95

Abstract

Cavity ring down spectroscopy (CRDS) is used to measure with unprecedented sensitivity and accuracy the weak water vapor spectrum in the 13171-13417 cm^{-1} region. A total of more than 1400 water lines are rovibrationally assigned to four isotopologues in natural isotopic abundance (H_2^{16}O , H_2^{18}O , H_2^{17}O and HD^{16}O), leading to the determination of 151 new levels and correction of 160 levels. The review of previous experimental works in the region is discussed. The comparison to the recent HITRAN2020 spectroscopic databases and to the W2020 line lists [Furtenbacher et al. J. Phys. Chem. Ref. Data 49 (2020) 043103; <https://doi.org/10.1063/5.0030680>] shows important discrepancies both for line positions and line intensities. A significant fraction of the W2020 line positions is inaccurate and shows deviations compared to measurements largely exceeding their claimed error bars. Line intensities are poorly predicted by available *ab initio* calculations in the considered region. A recommended line list mostly based on the present CRDS measurements is proposed.

1. Introduction

The present work takes part in long-standing efforts aiming at improving the knowledge of the absorption spectroscopy of the first greenhouse gas: water vapor. While high sensitivity laser techniques such as cavity ring down spectroscopy (CRDS) have been extensively used in the near infrared (see *e.g.* [1-3]), most of our knowledge of the water vapor spectrum in the visible ($\lambda < 800$ nm) relies on spectra recorded by Fourier transform spectroscopy with long multipass cells (*e.g.* [4-10]), or by intracavity laser spectroscopy (ICLAS) (*e.g.* [11,12]).

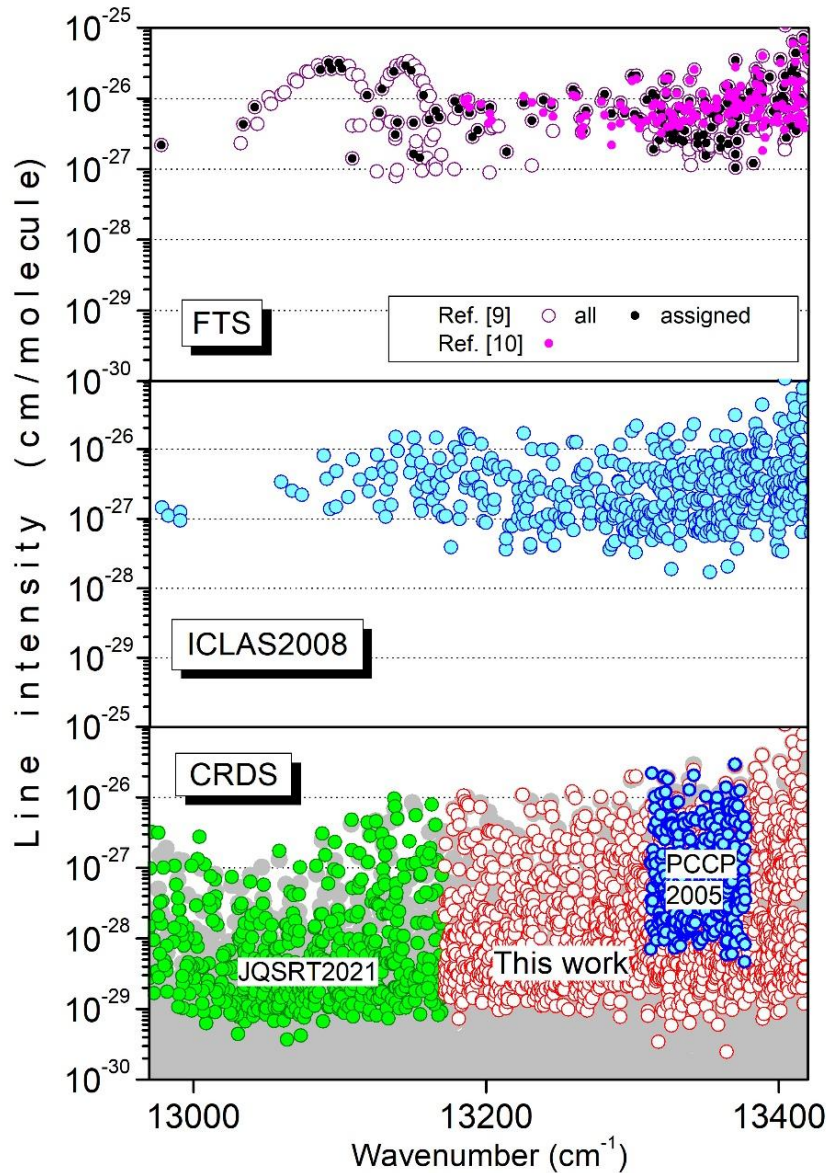


Fig. 1

Overview comparison of the FTS, ICLAS and CRDS line lists of H_2^{16}O between 12970 and 13420 cm^{-1} .

Upper panel: the FTS lists from Ref. [9] and Ref. [10] are superimposed (open circles and pink dots, respectively). The lines assigned to water in Ref. [9] are highlighted (black dots) - note the presence of the oxygen A-band transitions,

Middle panel: ICLAS [11],

Lower panel: CRDS studies of Ref. [13] and Ref. [14] (blue and green dots, respectively) and present work (red open circles). The HITRAN2020 list [15] is plotted in the background (grey symbols).

Fig. 1 illustrates the review of the most relevant experimental studies in the 12970-13420 cm^{-1} range, including the presently studied interval (13171-13417 cm^{-1}). Absorption lines are weak in this region with maximum intensity on the order of 10^{-25} $\text{cm}/\text{molecule}$ near 13400 cm^{-1} . Recently, using the same CRDS spectrometer [16] as used in the present work, recordings were dedicated to the lower part of the range (12970-13172 cm^{-1}) [14]. This spectral interval corresponds to the A-band of oxygen of particular importance for atmospheric applications and interfering lines of atmospheric water vapor have to be accurately characterized.

According to **Fig. 1**, the Fourier transform spectroscopy (FTS) technique coupled with a multi-reflection cell (absorption pathlength of several hundred meters) allows for the detection of lines with intensity above a few 10^{-27} $\text{cm}/\text{molecule}$ [9,10]. By providing effective absorption pathlengths of several tens km, a further gain in sensitivity by about a factor of five is achieved by ICLAS [11]. In 2005, we reported a first CRDS study in the region limited to the 13312-13378 cm^{-1} interval [13]. This specific interval was chosen as it corresponds to the region where Pfeilsticker et al reported the detection of water dimer absorption from low resolution spectra recorded in open air atmosphere with 18.4 km absorption path length over the sea [17]. The claimed water dimer signature was obtained by difference of the measured atmospheric absorbance and a simulation of the monomer absorption lines relying on the version of the HITRAN database available at that time. The sensitivity of the CRDS recordings of Ref. [13] allows for the detection of many new lines with intensity below 10^{-28} $\text{cm}/\text{molecule}$. The resulting additional absorbance of water vapor provided by these CRDS measurements was found to represent an important fraction of the reported water dimer absorption and questioned the reliability of the detection of water dimer in the atmosphere, which was finally revoked [18].

Due to the scarcity of previous measurements in the region, line parameters provided by spectroscopic database are mostly calculated *i.e.* line positions relying on empirical value of the upper and lower energy levels while line intensities have an *ab initio* origin [15]. With a detectivity threshold of about 10^{-29} $\text{cm}/\text{molecule}$, the present recordings with a noise equivalent absorption of about $\alpha_{\text{min}} \sim 5 \times 10^{-11}$ cm^{-1} give access to a high number of newly detected lines which can be used as validation tests of spectroscopic databases. In particular, we will consider (i) the so-called W2020 line lists of H_2^{16}O , H_2^{18}O and H_2^{17}O which are recommended by their authors to be included in the next generation of line-by-line spectroscopic information systems [19] and (ii) the current version of the HITRAN list in the region [15].

The rest of the report is organized as follows. The acquisition of the CRDS spectra is briefly described below together with the line list construction (Section 2). Section 3 includes the vibration-rotation assignments performed using known experimental energy levels and calculated water spectra based on variational calculations by Schwenke and Partridge (SP) [20-22]. Section 4 is devoted to a comparison to previous experimental studies and validation tests of the HITRAN2020 and W2020 lists.

2. Experiment

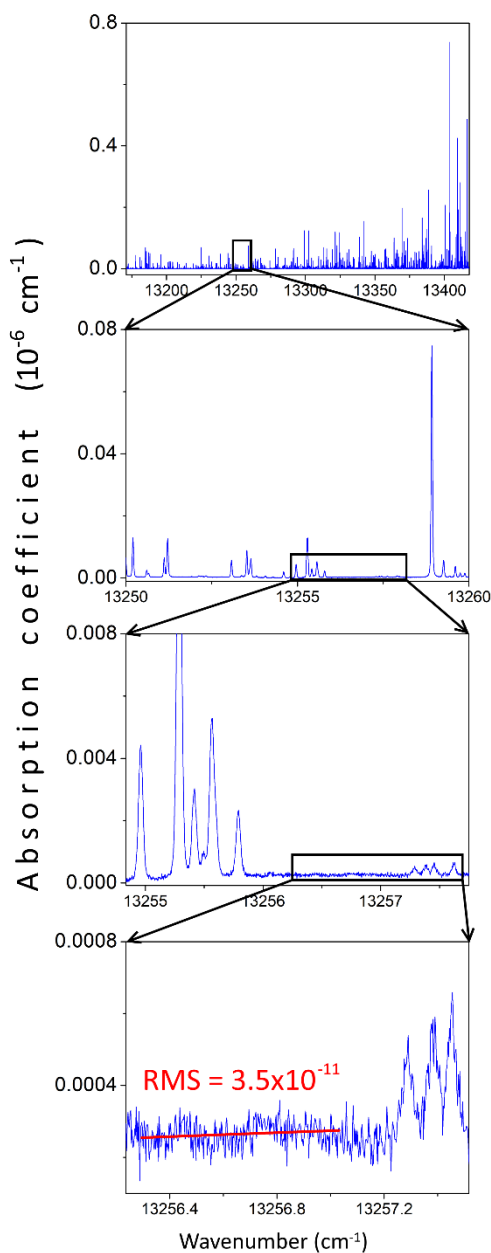


Fig. 2.

CRDS spectrum of water vapour at a pressure of about 9.5 Torr around 13250 cm^{-1} . The enlargements illustrate the dynamics achieved on the intensity scale and the noise equivalent absorption ($\alpha_{\min} \approx 5 \times 10^{-11}\text{ cm}^{-1}$). The three lines observed on the lower panel have an intensity smaller than $5 \times 10^{-29}\text{ cm/molecule}$.

The spectra were recorded with the CRDS spectrometer developed at the Institute of Atmospheric Optics in Tomsk [16]. The experimental arrangement and data acquisition are similar to those implemented in Grenoble [23,24]. Their description has been detailed in Ref. [14] and is not repeated here. Briefly, an external cavity diode laser (ECDL) from Sacher Lasertechnik, tunable in the 745-775 nm spectral range ($12900\text{-}13400\text{ cm}^{-1}$) was used as radiation source. A fiber-optic beam splitter directs 20% of the radiation to a wavelength meter (HighFinesse WS-U, 5 MHz resolution,

measurement frequency up to 400 Hz). The remaining 80% is directed to a fiber-optic acousto-optical modulator which interrupts the radiation input into the cavity. At the cavity output, the radiation is focused onto a silicon avalanche photodetector (Thorlabs APD410A) which measures the exponential decay of the intracavity field (ring-down).

The pressure measured by a capacitance gauge (10 and 50 Torr Inficon CDG020D gauges having the accuracy of 0.5% of reading) and the ring down cell temperature were monitored during the recordings with 10 k Ω thermistor TDK B57861S. The whole investigated region between 13171 and 13417 cm^{-1} was covered by a single recording session at a pressure of about 10 Torr. The total recording time was about 32 hours. Let us mention that the recorded spectra show a ten of narrow ($<0.13 \text{ cm}^{-1}$) spectral gaps corresponding to intervals where the ECDL source could not be tuned (the values of the spectral gaps are listed in the headings of the experimental list provided as Supplementary Material). During the whole measurement campaign the temperature varied between 296.75 and 298 K.

The frequency calibration provided by the wavemeter was refined by shifting the whole spectrum in order to match accurate positions of water lines available in the region. Due to the lack of accurate measurements, the position of some reference lines of the region were calculated using accurate empirical values of the upper energy levels derived in [14]. The accuracy of the reference positions is estimated to $1 \times 10^{-3} \text{ cm}^{-1}$, which is thus the estimated accuracy of the frequency scale of the spectra.

Fig. 2 illustrates the sensitivity and high dynamical range on the intensity scale. The noise equivalent absorption evaluated as the root mean square (*RMS*) of the baseline fluctuations is around $3.5 \times 10^{-11} \text{ cm}^{-1}$. The three lines displayed on the lower panel have an intensity smaller than $5 \times 10^{-29} \text{ cm/molecule}$.

The line centers and intensities were determined using an interactive least squares multi-lines fitting program written in LabVIEW. Most of the line profiles were assumed to be of Voigt type but for the strongest lines, the (obs. – calc.) residuals show the usual W-shape signature revealing the significance of collisional narrowing effects. The quadratic speed-dependent Nelkin-Ghatak profile was adopted to fit the observed profile and derive the line position and integrated absorption coefficient. The HWHM of the Gaussian component was fixed to the theoretical value of the Doppler width of H₂O (about 0.019 cm^{-1} half-width at half-maximum for H₂¹⁶O at 296 K near 13200 cm^{-1}). Note that at the 10 Torr pressure of the recordings, the Doppler width is larger than the self-pressure broadening (0.005- 0.01 cm^{-1} according to Ref. [15]). **Fig. 3** illustrates the quality of the spectrum fit near 13375 cm^{-1} .

Overall the global line list, displayed on the lower panel of **Fig. 1**, includes a total of 1420 entries between 13171.41 and 13417.81 cm^{-1} . The accuracy of the fitted line centers is estimated to be better than $3 \times 10^{-3} \text{ cm}^{-1}$ for unblended lines. This value includes the uncertainty on the calibration of

the frequency axis ($\sim 1 \times 10^{-3} \text{ cm}^{-1}$), the precision on the line center determination and the contribution of the small ($< 5 \times 10^{-4} \text{ cm}^{-1}$) unknown self-pressure shift of the line center [25].

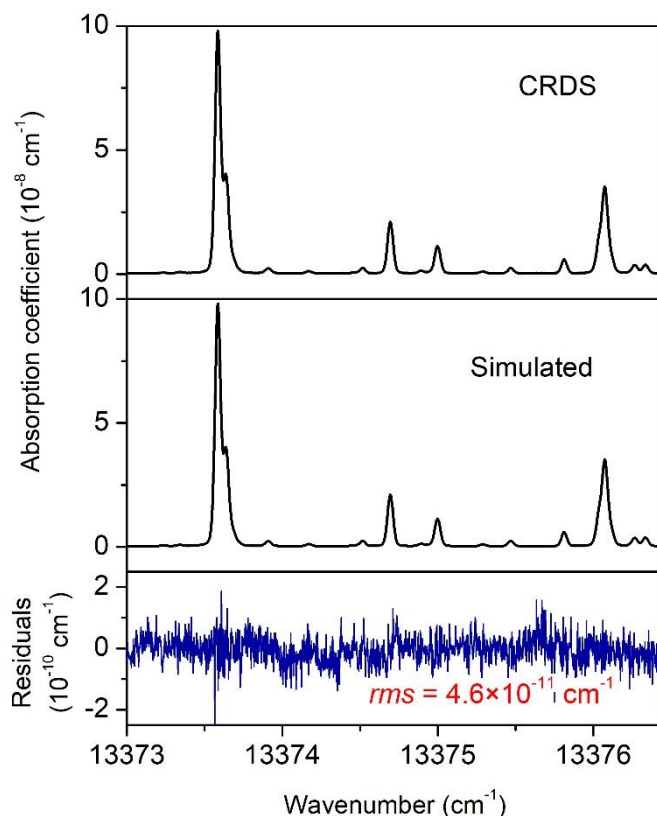


Fig. 3

Example of the quality of spectra reproduction provided by the line profile fitting. The pressure of water vapor was about 9.5Torr.

3. Rovibrational analysis

The rovibrational assignments were performed using the IUPAC empirical energy levels [26-28], the variational line list by Schwenke and Partridge (SP) [20-22] and the recent W2020 list [19]. Energy levels newly derived from the analysis in the oxygen A-band region were also considered [14]. 1412 lines were assigned to 1575 transitions of four water isotopologues (H_2^{16}O – 1257, H_2^{18}O – 61, H_2^{17}O – 4, and HD^{16}O – 253). The complete line list with rovibrational assignments is provided as Supplementary Material. At the end of the assignment procedure, eight lines with intensities smaller than $6.1 \times 10^{-29} \text{ cm/molecule}$ were left unassigned. No lines due to impurities were identified in the considered region.

For the main isotopologue, H_2^{16}O , 1139 lines were assigned to 1257 transitions. For comparison, 440 H_2^{16}O lines were previously assigned to 475 transitions by ICLAS [11] in the same region. The assigned transitions belong to 20 cold and eight hot bands. Let us underline the difficulties related to the vibrational labeling. The SP line list [22] was taken as basis because it is the only available variational list that gives complete vibration-rotation labeling for all calculated transitions. However, it should be mention that the same vibration-rotation labeling is sometimes attached to

various SP energy level which makes the assignment ambiguous. The complexity of the vibrational labeling is due to the fact that about 30 vibrational bands fall into the studied range. The rotational levels of most vibrational states are strongly mixed, so the vibrational labeling is often ambiguous. In general, the deviations of SP calculated line positions from the observed values have smooth vibration and rotation dependences. These dependences *versus* J and K_a allow for assigning new energy levels when a sufficient series of deviations is available from already known levels.

The problem of the studied spectral range is the reduced number of energy levels for the vibrational states of interest, especially those with a large excitation of the bending vibration: (061), (080), (090), (160), (170), (250), etc. On the other hand, as noted in previous studies (see, for example, Refs. [14,29]), strong resonance perturbations can break the smooth dependences of deviations and some of the vibrational labeling remain ambiguous.

The absorption spectrum of H_2^{18}O in the region was studied by Leshchishina et al. [29] by ICLAS of a highly ^{18}O enriched sample. 61 transitions of H_2^{18}O in natural isotopic abundance are identified in the present spectra. They belong to six bands ($\nu_1+4\nu_2+\nu_3$, $2\nu_1+2\nu_2+\nu_3$, $2\nu_1+4\nu_2$, $3\nu_1+\nu_3$, $3\nu_1+2\nu_2$, and $4\nu_1$). Measured line positions are in good agreement with the results of Ref. [29]. The $\delta\nu = |\nu^{\text{TW}} - \nu^{\text{Ref. [28]}|$ deviations exceed 0.01 cm^{-1} only for seven lines. The *RMS* deviation is 0.0065 cm^{-1} with maximum discrepancy of 0.0222 cm^{-1} for the $3\nu_1+\nu_3$ $13_1 13 - 14_1 14$ line position at $13403.5837 \text{ cm}^{-1}$ which is blended by the much stronger line $2\nu_1+2\nu_2+\nu_3$ $10_0 10 - 10_2 9$ of the main isotopologue. Note that the estimated experimental uncertainties of the line positions in Ref. [29] are between 0.005 and 0.015 cm^{-1} .

Absorption lines of the HD^{16}O isotopologue were reported in Refs. [10,30-32] in the region of interest. In our analysis, 253 HD^{16}O transitions of the $2\nu_2+3\nu_3$ and $\nu_1+3\nu_3$ bands were identified. The corresponding line positions are in good agreement with previous studies [10,30-32]. Compared to the ICLAS study of Ref. [32], the position differences $\delta\nu = |\nu^{\text{TW}} - \nu^{\text{Ref. [32]}|$ are larger than 0.01 cm^{-1} for only 17 transitions. The *RMS* deviation is 0.0059 cm^{-1} with maximum discrepancy of 0.0259 cm^{-1} for the $2\nu_2+3\nu_3$ $4_2 2 - 4_1 3$ line position at $13317.2251 \text{ cm}^{-1}$. The line position of this transition is very close to those of the $\nu_1+3\nu_3$ $3_2 2 - 3_2 1$ transition at $13317.2616 \text{ cm}^{-1}$. These two lines were not resolved in Ref. [32]. Estimated experimental uncertainties of the line positions in Ref. [32] are the same as those of Ref. [29] for H_2^{18}O (between 0.005 and 0.015 cm^{-1}).

In addition, three $2\nu_1+2\nu_2+\nu_3$ and one $3\nu_1+2\nu_2$ transitions of H_2^{17}O isotopologue were assigned in our CRDS spectrum of natural water.

4. Comparison to literature data

4.1 Experimental line lists

As mentioned above, due to the weakness of the water absorption lines in the region, previous experimental studies are scarce (see **Fig. 1**). The two most relevant FTS studies were obtained by the Reims–Brussels collaboration at a spectral resolution of 0.06 cm^{-1} with a total absorption path length

up to 602.32 m [4] and at the Rutherford Appleton Laboratory (RAL) with path lengths up to 800.8 m and a spectral resolution of 0.03 cm^{-1} [6-10]. The RAL spectra were analyzed in Tolchenov et al. [9] but the line list attached to this reference includes assignment errors and artifacts which were corrected in Ref. [10] (see upper panel of **Fig. 1**). Overall the Reims-Brussels [4] and RAL spectra [10] have a similar sensitivity (about 180 and 150 detected lines in our region, respectively).

The ICLAS study of Ref. [11] provided a higher sensitivity allowing to increase the number of measured lines to more than 440 (assigned to 475 transitions of the main isotopologue). Note that the weakest lines measured by ICLAS have an intensity of about $10^{-27} \text{ cm/molecule}$, two orders of magnitude above the detectivity threshold of the present CRDS recordings (**Fig. 1**).

All but five ICLAS lines are confirmed by the present CRDS recordings. The lines at 13245.7856 and $13402.3457 \text{ cm}^{-1}$ reported with no assignments in Ref. [11] are also confirmed and correspond to the $9\nu_2 5_{23} - 6_{34}$ and $2\nu_1 + 3\nu_2 + \nu_3 - \nu_2 4_{22} - 5_{23}$ transitions respectively. The *RMS* value of the differences ($\delta\nu = \nu^{CRDS} - \nu^{ICLAS}$) is 0.0077 cm^{-1} with maximum deviations up to 0.035 cm^{-1} . The differences $\delta\nu$ exceed 0.02 cm^{-1} for the nine weakest lines. This is consistent with the uncertainty of 0.004 cm^{-1} on the ICLAS line positions [11] combined to the present 0.003 cm^{-1} estimated uncertainty on the CRDS values.

4.2 W2020 line positions

Following the approach developed a decade ago by a task group (TG) of the International Union of Pure and Applied Chemistry (IUPAC) [26-28], most of W2020 line positions [19] rely on empirical energy levels derived from an exhaustive collection and review of measured transitions [19,33]. These empirical energy levels and line positions are tagged with “M” in the W2020 lists [19]. In absence of empirically determined energy levels, less accurate calculated values are used (tag “C”). The procedure and code xMARVEL were applied to the constructed catalog of published absorption and emission measured line positions of H_2^{16}O , H_2^{18}O and H_2^{17}O and recommended sets of empirical energy levels were released with their self-consistent uncertainties [19]. For the main isotopologue, the W2020- H_2^{16}O transition dataset gathers 286,987 non-redundant rovibrational transitions, and 19,225 empirical energy levels were determined [19].

In a recent contribution, we presented validation tests of the W2020 positions in the $8040\text{-}8630 \text{ cm}^{-1}$ region and concluded that, in the considered region, “the sophisticated xMARVEL procedure and algorithm elaborated to identify and adequately weight inaccurate line positions among the large W2020 transition database do not always prevent less accurate data from “spoiling” higher quality data sources” [31]. In other words, spectra newly recorded in Ref. [31]) (by CRDS) confirmed the quality of some experimental lists of the literature which were included in the W2020 transition database but the xMARVEL treatment led to recommended W2020 positions less accurate than these published original sources. In addition, some position deviations were found to exceed the W2020 claimed uncertainty on the transition frequencies by large factors ($>10\text{-}100$) [34].

Similar conclusions were drawn in the region of the A-band of O₂ (12970-13200 cm⁻¹) [14,34] where previous observations are much scarcer than in the near infrared. A number of substantial position deviations were evidenced, and in many cases, the W2020 error bars appeared to be strongly underestimated.

In the spectral region of present interest, located just above the A-band region, the situation is similar to that encountered in the two above regions. The series of six examples presented on **Fig. 4** illustrate some position discrepancies between the observations and the W2020 (and HITRAN2020) lists. Note the position differences between the W2020 and HITRAN2020 positions observed in the intervals displayed in **Figs. 4 a-c-d** which will be discussed below.

In order to provide a systematic comparison between the W2020 line list and our measurements, corresponding transitions in the different lists have to be identified. Identical lower state and upper J values, close values of the positions and intensities (within 0.3 cm⁻¹ and 20-30 %, respectively) and the rovibrational assignment (when available) were used as criteria. In fact, as it was shown in Ref. [14], the criterion of the intensity proximity in this spectral range is not always fulfilled. One such example is shown in Fig. 4a. The experimental intensity value of the $2\nu_1+4\nu_2$ $1_{11} - 0_{00}$ line at 13262.5888 cm⁻¹ is 1.87×10^{-27} cm/molecule, while the calculated values in two different lists are 3.066×10^{-27} cm/molecule [19] and 5.682×10^{-28} cm/molecule [15]. A significant number of the W2020 transitions are provided without vibrational labeling of the upper level and without K_a and K_c values (only the J value is given). In the global list provided as Supplementary Material, for each measured transition, the corresponding W2020 position and intensity values are given (except for the HD¹⁶O isotopologue). Note that the vibrational labeling of about 200 W2020 transitions had to be modified or completed. The list includes the original W2020 assignments [19] when they have been changed. The HITRAN2020 values are also included together with the HITRAN reference codes for the line positions and line intensities.

The W2020 uncertainties on the line positions plotted in **Fig. 4**, are considerably smaller than the deviations from the measured line centers. The stick spectra corresponding to the ICLAS [11] and CRDS [13] literature studies are included in the figure (cyan and black symbols, respectively). The present CRDS measurements confirm the quality of these two previous experimental line lists which are both part of the W2020 transition database [19]. Unexpectedly, in the displayed examples, the W2020 recommended position values differ significantly from the published ICLAS [11] and CRDS [13] values, probably due to the impact of other experimental sources of lower quality, also included in the W2020 transition database. These examples confirm the deficiencies of the xMARVEL global procedure and algorithm in identifying and adequately weighting inaccurate line positions among the large W2020 transition database.

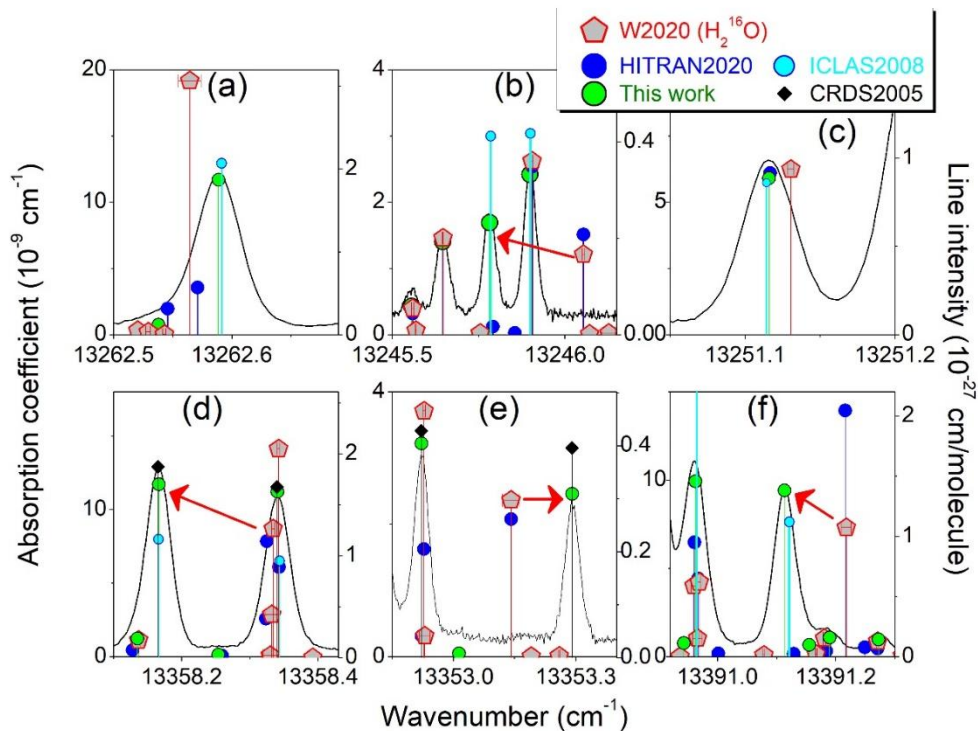


Fig. 4

Examples of comparison of the CRDS spectrum of water vapor and corresponding line list (green circles) to the W2020 line list of H_2^{16}O [19] (grey pentagons) and the HITRAN2020 list of natural water [15] (blue circles). In the cases of line positions based on empirically determined energy levels, the W2020 error bars are displayed. The right-hand intensity scale is adjusted to correspond approximately to the peak heights.

Considering the W2020 H_2^{16}O positions relying on empirical energy levels (“M” positions), 978 transitions are in common with our measurements. The corresponding average and *RMS* values of the position differences ($\delta V = \nu_{CRDS} - \nu_{W2020}$) are -0.00644 and 0.0591 cm^{-1} , respectively. These values should be taken with cautious as they are affected by a number of large outliers. For instance, the W2020 position of the $7\nu_2+\nu_3 \ 11_{111} - 12_{310}$ transition ($13340.5697 \text{ cm}^{-1}$) is larger than the experimental value ($13339.4912 \text{ cm}^{-1}$) by 1.0785 cm^{-1} . This deviation is about 900 times the error bar of 0.0012 cm^{-1} of the W2020 position. This is the most extreme example of underestimation of the W2020 position uncertainties.

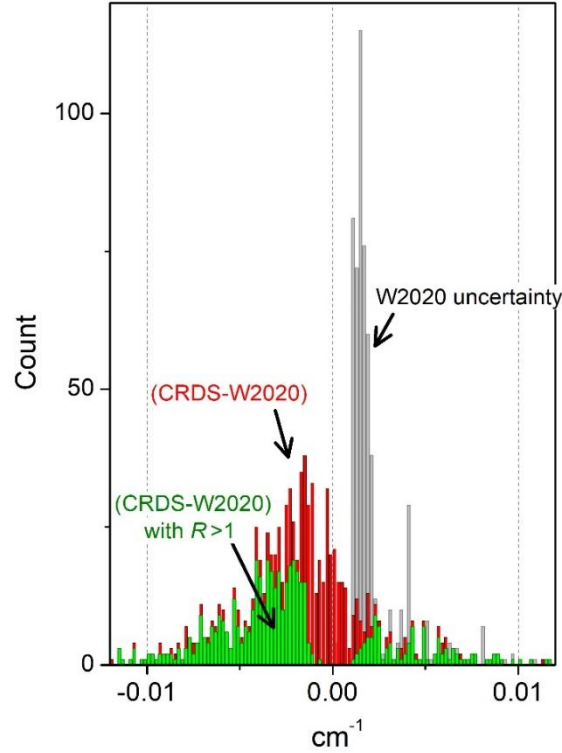


Fig. 5

Histogram of the position differences between the CRDS line positions of H_2^{16}O measured in the $13171.41 - 13417.81 \text{ cm}^{-1}$ interval and the corresponding W2020 value [19] (red). The green bars correspond to the histogram of the position differences exceeding the W2020 position uncertainty ($R > 1$). The histogram of the W2020 uncertainties is given for comparison (grey bars).

The histograms of **Fig. 5** provide a more general view of the situation. For example, the W2020 positions appear to be on average systematically overestimated by about $1.5 \times 10^{-3} \text{ cm}^{-1}$. The ratio $R = \frac{|v_{\text{CRDS}} - v_{\text{W2020}}|}{\text{Unc}_{\text{W2020}}}$ which compares the absolute deviation of the W2020 position from the CRDS value to the claimed W2020 position uncertainty can be obtained from the global list provided as Supplementary Material. The histogram corresponding to transitions with position deviation exceeding the claimed W2020 uncertainty ($R > 1$) is included in **Fig. 5** (green bars). Among the 978 W2020 empirical positions, 559 have a R value larger than 1. Among these, 396 deviate by more than the uncertainty on the present CRDS measurements ($3 \times 10^{-3} \text{ cm}^{-1}$).

The histogram of the W2020 position uncertainties is included in **Fig. 5** (grey bars). Most of W2020 error bars are between 1 and $2 \times 10^{-3} \text{ cm}^{-1}$ (the minimum uncertainty value is $2 \times 10^{-4} \text{ cm}^{-1}$). These values are significantly smaller than the position uncertainties claimed in the two literature studies providing most of the experimental information by absorption in the region ($4 \times 10^{-3} \text{ cm}^{-1}$ by ICLAS [11] and $5 \times 10^{-3} \text{ cm}^{-1}$ by CRDS [13]). The W2020 empirical positions rely thus not only on the ICLAS measurements but also on energy levels retrieved from measurements performed in different spectral regions, in particular less accurate emission spectra [19]. The complexity of the xMARVEL procedure and the large number of sources make difficult to trace precisely the origin of the W2020 inaccuracies.

4.3 HITRAN2020 line positions

According to the reference codes attached to the line positions of the HITRAN list, the HITRAN2020 database adopted the W2020 empirical transition frequencies from Ref. [19] for H_2^{16}O , H_2^{17}O and H_2^{18}O . Otherwise, variational values of Bubukina et al. [35] were adopted, mostly for (weak) lines with upper state energy level not yet determined by experiment. In fact, for unknown reasons, we evidenced significant differences between HITRAN2020 and the W2020 original line list:

(i) a fraction of the HITRAN2020 transitions with claimed W2020 origin differs importantly from the original W2020 values of [19]. Among those, some HITRAN2020 line positions agree better with the experiment than the W2020 (empirical) line positions. A list of 55 such transitions is provided as Supplementary Material. Interestingly, we note that not all the W2020 empirical line positions were transferred to the HITRAN2020 list. For instance, the $6\nu_2+\nu_3\ 11_{6\ 5} - 12_{6\ 6}$ transition measured at $13312.8798\ \text{cm}^{-1}$ has a W2020 empirical position overestimated by $0.6125\ \text{cm}^{-1}$ (the W2020 uncertainty $0.0017\ \text{cm}^{-1}$ leads to a R value of 360). In the HITRAN2020 list, the calculated position value from Ref. [35] ($13312.9472\ \text{cm}^{-1}$) was judiciously preferred for this transition, leading to a position deviation from the measurement significantly reduced ($-0.0674\ \text{cm}^{-1}$).

(ii) some lines with significant intensity ($>5\times 10^{-28}\ \text{cm/molecule}$) are observed by CRDS and included in the W2020 list but missing in the HITRAN list. Some examples of these missing lines are included in the above Supplementary Material.

The origin of the evidenced problems affecting the HITRAN2020 list should be clarified and might possibly lead to an update of the HITRAN2020 list.

4.4 HITRAN2020 and W20200 line intensities

Let us recall that all the W2020 intensities are calculated values from the POKAZATEL list [36]. The HITRAN intensities are computed values of Ref. [37] except for the strongest lines of the region for which FTS intensities from Ref. [10] were preferred. Differences between the calculated intensities of the HITRAN2020 and W2020 lists reflect the sensitivity of the calculation to small changes in the potential energy or dipole moment surfaces in the considered region. This is probably related to the high excitation of part of the involved upper levels and to the fact that many of them involve a high bending excitation. A number of spectral intervals showing important disagreement between the experimental spectrum and the HITRAN2020 and W2020 line intensities are displayed in **Fig. 6**. It is amazing to note that in the displayed examples, the HITRAN2020 and W2020 line intensities are very different but neither agrees with the observations. This seems to reflect the high “instability” of the considered calculated line intensities, a small change of the potential energy surface used for the calculations leading to a large variation of the considered intensities.

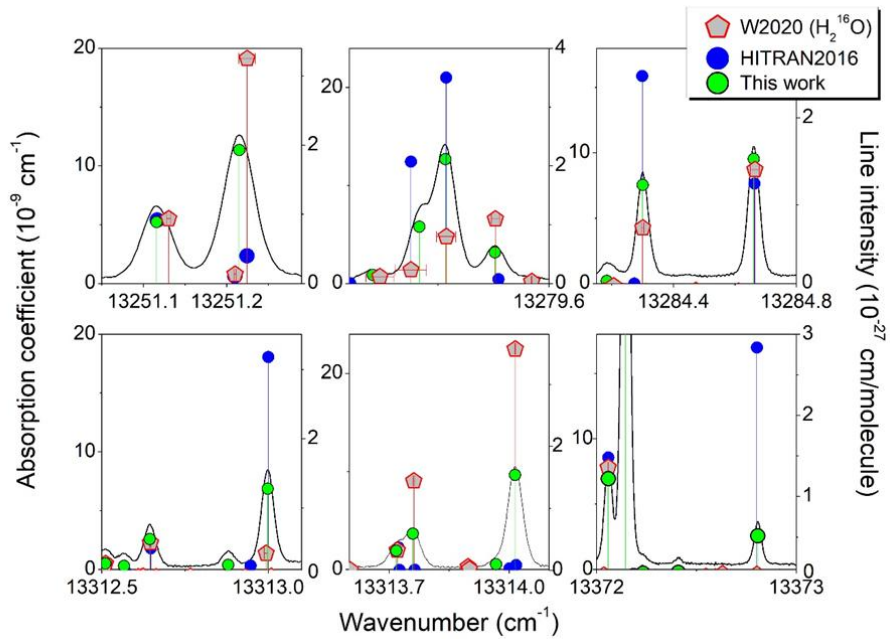


Fig. 6

Examples of comparison of the CRDS spectrum of water vapor and corresponding line list (green circles) to the W2020 line list of H_2^{16}O [19] (grey pentagons) and the HITRAN2020 list of natural water [15] (blue circles). The right-hand intensity scale is adjusted to correspond approximately to the peak heights. Note the large differences between the displayed W2020 and HITRAN2020 intensity values which are both computed values (see text).

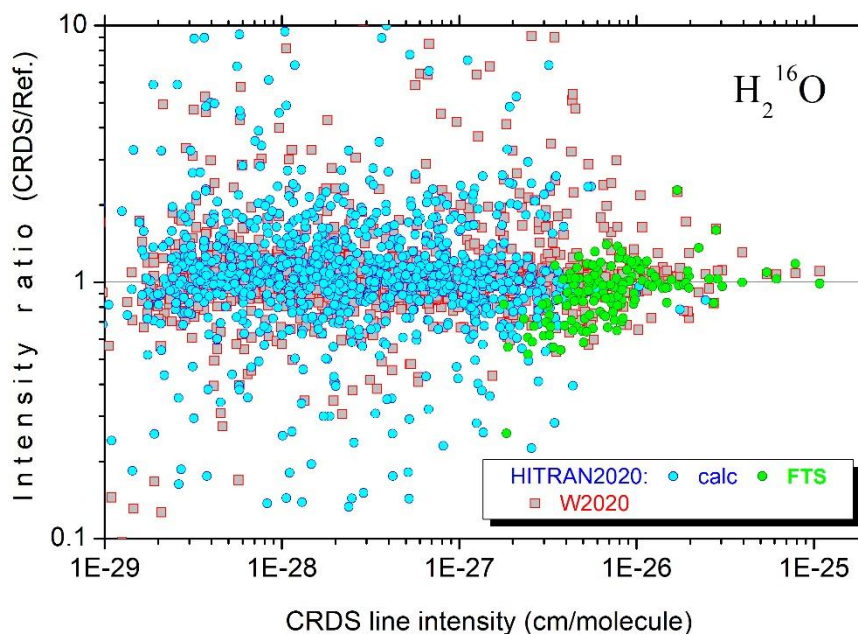


Fig. 7

Ratios of the CRDS values to the HITRAN2020 [15] and W2020 [19] intensities for H_2^{16}O transitions measured in the $13171.41 - 13417.81 \text{ cm}^{-1}$ (circles and squares, respectively), versus the CRDS intensity values. HITRAN values are either calculated values from Ref. [37] or FTS values from Ref. [10] (blue and green circles, respectively). Note the logarithmic scale adopted for the two axis.

The ratios of the present CRDS intensity values to the HITRAN2020 and W2020 intensity values are displayed in **Fig. 7**. Different symbols are used according to the HITRAN intensity source (FTS [10] or calculated [37]). A logarithmic scale is adopted both for the ratios and intensities axis. A large dispersion is noted both for HITRAN2020 and W2020 ratios. In general, the largest HITRAN outliers correspond to large intensity overestimations while in the case of the W2020 list, the largest outliers are due to strongly underestimated line intensities.

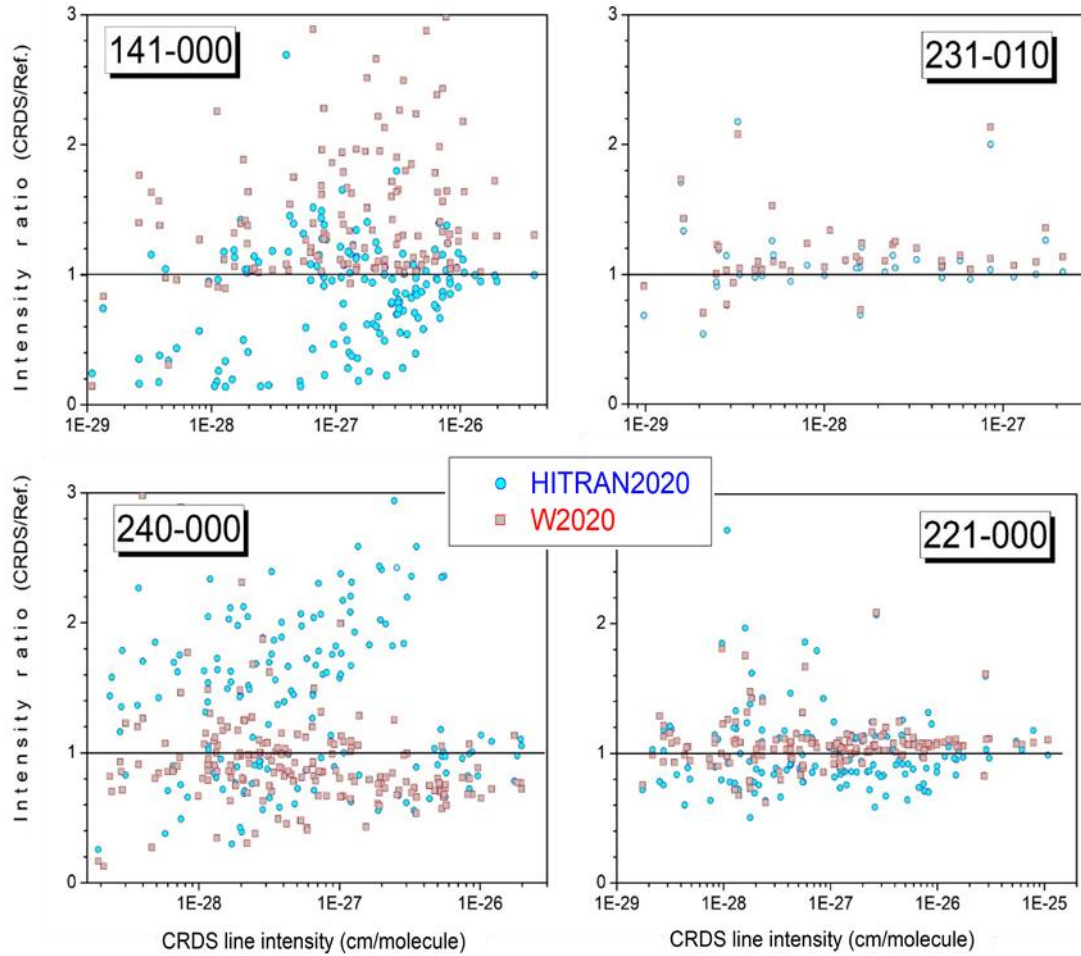


Fig. 8

Ratios of the CRDS values to the HITRAN2020 [15] and W2020 [19] intensities for H_2^{16}O transitions (cyan circles and red squares, respectively), *versus* the CRDS intensity values. Note the logarithmic scale adopted for the two axis. The W2020 intensity values are the POKAZATEL values of Ref. [36] intensities. The selected bands are $\nu_1+4\nu_2+\nu_3$ (*upper left*), $2\nu_1+3\nu_2+\nu_3-\nu_2$ (*upper right*), $2\nu_1+4\nu_2$ (*lower left*) and $2\nu_1+2\nu_2+\nu_3$ (*lower right*)

The ratios corresponding to the line intensities of some bands have been separated on four panels in **Fig. 8**. In the case of the $2\nu_1+3\nu_2+\nu_3-\nu_2$ hot band (upper right panel), the HITRAN2020 [37] and POKAZATEL [36] intensities are close and agree with the experimental values, although a systematic shift of about +3.2% and +10.4% is noted for HITRAN2020 and POKAZATEL, respectively. Despite the fact that the systematic shift for the two lists differs by more than three times, the *RMS* deviations are almost the same: 23.9% and 21.4% for HITRAN2020 and POKAZATEL,

respectively. The observed dispersion on the ratios provides a validation of the claimed uncertainty of the experimental intensities of about 5% for most of the lines. In the case of three other bands ($\nu_1+4\nu_2+\nu_3$, $2\nu_1+4\nu_2$ and $2\nu_1+2\nu_2+\nu_3$), the experimental intensities are intermediate between the two calculations but the difference are much larger. For example, for the $\nu_1+4\nu_2+\nu_3$ band (upper left panel), the POKAZATEL intensities of the W2020 list are about twice smaller than measured while the HITRAN2020 values are on average 50% larger than measured. The fact that both calculations show a better agreement with measurements for the $2\nu_1+2\nu_2+\nu_3$ (lower right panel) and $2\nu_1+3\nu_2+\nu_3-\nu_2$ (upper right panel) bands and a worse agreement for the $\nu_1+4\nu_2+\nu_3$ (upper left panel) and $2\nu_1+4\nu_2$ (lower left panel) bands, may indicate that the latter are more sensitive to small changes of the potential energy or dipole moment surfaces due to a higher vibrational excitation of the bending mode V_2 .

5. Energy levels

As concerns the upper energy levels (or term values), the positions of the lines assigned in the studied region allow us to determine 1124, 68, 4 and 124 term values for the H_2^{16}O , H_2^{18}O , H_2^{17}O and HD^{16}O isotopologues, respectively. The term values were obtained by adding lower state energy from Refs. [26-28]. Among the 1320 derived energy levels, 151 H_2^{16}O levels are newly determined (**Table 1**). A total of 160 H_2^{16}O energy levels were found to deviate by more than $5 \times 10^{-3} \text{ cm}^{-1}$ compared to the W2020 values [18] and have to be significantly corrected. **Table 2** compares their experimental and W2020 term values. In addition, 20 H_2^{18}O term values and three H_2^{17}O ones are differ from those of W2020 by more than 0.005 cm^{-1} .

We provide as a separate Supplementary Material the list of upper energy levels of H_2^{16}O , H_2^{18}O , H_2^{17}O and HD^{16}O derived in this work ($13170\text{-}13418 \text{ cm}^{-1}$) and in the oxygen A-band region ($12969\text{-}13170 \text{ cm}^{-1}$) [14]. About 40% of energy levels were derived using several transitions assigned in the $12969\text{-}13418 \text{ cm}^{-1}$ sharing the considered upper state. Ground state combination difference (GSCD) relations can be used to estimate the accuracy of the determined upper energy levels. The *RMS* of the differences between independent determinations of the upper energy level is $2.4 \times 10^{-3} \text{ cm}^{-1}$. These values are consistent with the claimed uncertainty of $3 \times 10^{-3} \text{ cm}^{-1}$ on the reported line positions.

The supplementary material provides also a comparison to the W2020 empirical energy levels (except for HD^{16}O), with the corresponding $R = \frac{|E_{\text{CRDS}} - E_{\text{W2020}}|}{\text{Unc}_{\text{W2020}}}$ values. For the main isotopologue, among the 1124 term values derived from the spectra analysis in the overall $12969 - 13418 \text{ cm}^{-1}$ region (this work and Ref. [14]), 238 are newly determined (*i.e.* they have variational origin in the W2020 dataset – label "C") and 548 shows deviations compared to W2020 (empirical) values larger than the W2020 uncertainty ($R > 1$). Most of the W2020 empirical values are larger than our values and for about 30 of them the deviation exceeds 0.1 cm^{-1} . Note that we provide a complete and unique labeling for all the energy levels including for 238 energy levels with incomplete W2020 labeling. The W2020 labeling of 30 levels has been changed.

6. Recommended line list

In the infrared range, except for some specific bands, variational intensities of water vapor transitions show an overall good agreement with experimental data. In the considered range near 750 nm, the available calculated line lists (SP [20-22], Conway et al. [37] in HITRAN2020 and POKAZATEL [36] in W2020) show a large dispersion of the computed intensity values and neither of them shows a satisfactory agreement with the measurements (**Figs. 6-8**). For example, SP list contains about relatively strong transitions of the order of 10^{-27} cm/molecule of bands with a large bending excitation ($9\nu_2$, $8\nu_2$, $\nu_1+6\nu_2$, $6\nu_2+\nu_3$) that are not observed in the spectrum in spite of a detectivity threshold on the order of 10^{-29} cm/molecule. The SP intensity of these lines are thus believed to be strongly overestimated. Large deviations from the observations are also noted for some highly excited bands of the bending mode ν_2 in the W2020 line list (see **Fig. 8**). The above comparisons indicate that the basis of a recommended line list in the region must thus be experimental, both for line positions and line intensities. The recommended line list provided as Supplementary Material relies mostly on the CRDS line parameters derived in this work. The intensity cut off is fixed to 1×10^{-29} cm/molecule. Overall, the list includes 2050 transitions of four most abundant isotopologues of water (H_2^{16}O , H_2^{18}O , H_2^{17}O and HD^{16}O) in natural isotopic abundance.

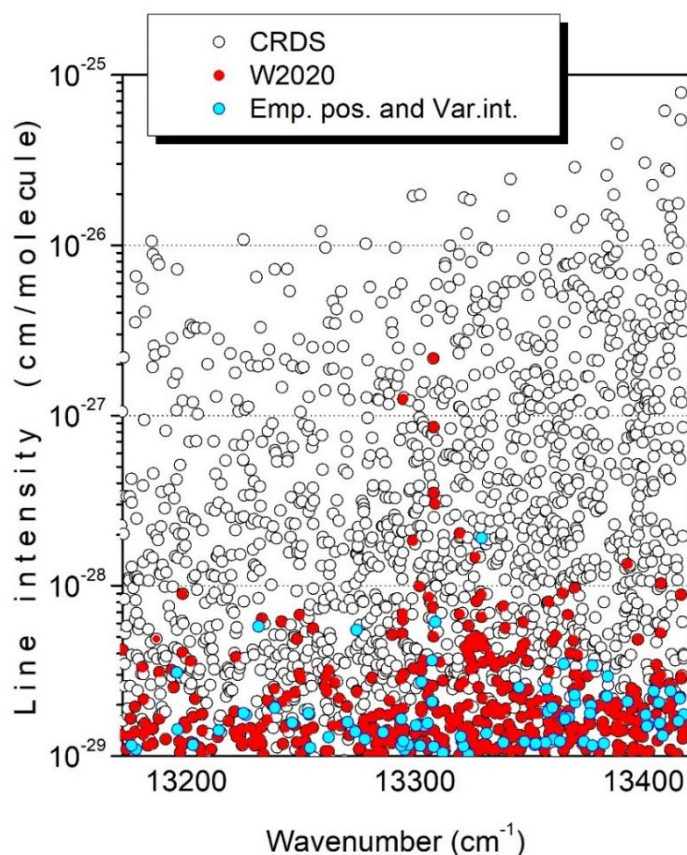


Fig. 9

Absorption line list for water vapour in natural isotopic abundance recommended for the 13170 – 13418 cm^{-1} spectral interval. In the narrow spectral intervals missing CRDS spectra and for weak lines obscured by much stronger lines, the CRDS list has been completed with transitions with empirical positions (cyan dots) and W2020 transitions [19] (red dots). The intensity cut off is fixed to 1×10^{-29} cm/molecule.

In the narrow spectral intervals missing CRDS spectra and for weak lines obscured by much stronger lines, the list was completed with transitions with empirical positions when possibly associated to W2020 intensities for H₂¹⁶O, H₂¹⁸O and H₂¹⁷O species and SP intensities for HD¹⁶O (labels “w” and “s”, respectively). A total of 473 transitions were added in this way. 168 of these 473 transitions with W2020 variational line positions (line position uncertainty “-9999”) and incomplete vibration-rotation assignment had to be included to achieve completeness. We tried to check that these W2020 added transitions were compatible with the spectra at disposal (some lines with calculated intensity clearly above our detectivity threshold were excluded) but, considering the quality of the W2020 positions and intensities, these added lines should be considered with cautious. The sources of the line parameters which are given for each transition in the Supplementary material, are indicated on the overview presented in **Fig. 9**.

7. Concluding remarks

The present study in the 13170 – 13418 cm⁻¹ interval has extended to higher energy our preceding study of the water vapor absorption in the region of the oxygen A-band near 760 nm (12969 – 13170 cm⁻¹) [14]. The reported results were obtained on the basis of high sensitivity CRDS recordings which improved by two orders of magnitude the sensitivity of previous observations by ICLAS [11]. The constructed recommended line list will allow to improve the spectroscopic databases in the region. 151 H₂¹⁶O levels were newly determined (**Table 1**) while 160 additional energy levels were found to deviate by more than 5×10⁻³ cm⁻¹ compared to the W2020 values [19]. The detailed comparison with the W2020 line positions has confirmed the conclusions drawn near 1.25 μm [34] and in the A-band region [14]:

(i) for a large fraction of transitions, the procedure xMARVEL used to determine the empirical W2020 energy levels by inversion of a large transition dataset available from the literature leads to values which are less accurate than some of the used experimental sources. In the present case, part of the W2020 recommended position values differ significantly from the published ICLAS [11] and CRDS [13] values while the quality of these previous studies is confirmed by the present measurements (see **Fig. 4**).

(ii) the uncertainty values attached to the W2020 empirical positions and energy levels are not reliable. The histograms of **Fig. 5** indicate that for about half of the line positions, the deviation from the measured values exceeds the W2020 claimed error bar ($R = \frac{|v_{CRDS} - v_{W2020}|}{Unc_{W2020}} > 1$). R values larger than 10 are observed (see **Table 2**).

According to the HITRAN2020 database, the W2020 empirical positions of Ref. [19] was adopted as the main source of line positions in the region. In fact, significant differences between HITRAN2020 and the W2020 original line list have been evidenced in this work, some of them leading to a better agreement with the measurements. The origin of this situation should be clarified and might possibly lead to an update of the HITRAN2020 list. We also noted that some lines with

significant intensity ($>5 \times 10^{-28}$ cm/molecule) are observed in the CRDS spectra and included in the W2020 list but missing in the HITRAN2020 list.

Acknowledgements

The support of the CNRS (France) in the frame of International Research Project SAMIA is acknowledged. CRDS measurements and spectrum analysis were performed at IAO-Tomsk and funded by Ministry of Science and High Education of the Russian Federation.

Table 1

Energy levels of H₂¹⁶O firstly determined from the analysis of the CRDS spectra of water vapor between 13170 and 13418 cm⁻¹.

$V_1V_2V_3$	J	K_a	K_c	Energy (cm ⁻¹)	$V_1V_2V_3$	J	K_a	K_c	Energy (cm ⁻¹)	$V_1V_2V_3$	J	K_a	K_c	Energy (cm ⁻¹)
023	9	2	7	15258.7584	122	10	2	8	15330.5429	240	10	3	8	14774.2742
023	12	2	11	15785.4447	122	11	2	9	15796.3450	240	10	3	7	14835.5360
032	10	2	8	15530.7288	122	11	3	9	15797.6128	240	10	4	6	15002.1090
042	2	1	1	13566.4404	122	11	4	7	15531.1616	240	10	5	5	15237.8770
042	4	4	0	14136.6087	122	12	3	10	15532.0568	240	11	1	11	14475.8195
042	6	5	1	14618.1513	141	7	4	3	14391.5188	240	11	4	7	15262.7430
042	9	1	9	14347.1330	141	10	4	7	15028.0751	240	12	0	12	14710.0991
042	9	2	8	14585.6731	141	11	3	8	15166.7499	240	13	1	13	14916.6936
042	9	5	5	15194.1251	141	11	6	5	15618.0617	240	13	3	10	15187.0823
042	10	5	5	15424.2091	141	11	7	5	15942.4378	240	13	5	8	15727.7784
042	11	2	9	15228.0496	141	12	6	7	16028.0637	240	14	1	14	15167.5190
042	11	3	9	15265.1230	141	12	6	6	16031.0931	250	2	2	1	14854.0580
042	11	4	8	15482.7875	151	4	4	0	15476.4282	250	3	2	1	14923.3118
042	11	4	7	15496.1661	160	4	4	0	13575.1211	250	4	2	3	15014.9853
042	11	5	7	15699.6539	160	5	4	1	13694.1945	250	6	2	5	15262.8063
042	11	5	6	15686.1290	160	5	5	0	14035.7733	301	11	5	7	15632.5117
042	12	3	10	15553.7978	160	6	3	4	13529.2240	301	11	6	5	15795.5404
042	12	4	8	15824.8627	160	6	5	1	14180.8768	301	11	7	4	15905.4097
042	13	3	10	15978.7537	160	7	3	5	13694.9521	301	11	8	4	16091.4874
042	13	5	8	16329.2381	160	7	5	3	14349.2370	301	11	8	3	16091.2795
061	4	4	1	13631.4480	160	8	5	4	14540.5148	301	11	9	3	16280.0041
061	5	3	3	13462.8335	160	8	5	3	14540.9104	301	11	9	2	16280.0044
061	6	4	3	13896.4804	160	9	3	6	14095.8421	301	12	5	7	15935.2574
061	6	5	2	14212.8961 ^a	160	9	4	5	14395.8694	301	12	7	6	16181.3603
061	7	4	4	14064.5510 ^b	160	9	5	4	14754.5167	301	12	7	5	16181.7481
061	7	4	3	14060.5410	160	11	2	9	14377.0873	301	13	3	10	16097.2759
061	8	4	4	14250.9054	160	11	4	7	14865.4675	301	13	4	9	16195.4118
061	9	5	5	14793.0208	160	12	2	10	14648.8477	301	13	5	8	16246.1654
061	10	6	4	15356.2534	160	14	5	10	16141.8591	301	14	2	12	16209.8547
061	11	2	9	14493.6292	170	8	0	8	14483.2750	301	16	1	15	16578.9259
061	11	5	7	15291.3205	170	9	1	9	14756.9365	320	10	1	9	15170.1657
061	13	5	9	15885.7780	221	11	5	6	15710.2282	320	10	4	6	15227.1380
071	10	1	10	15086.6849	221	12	3	10	15568.1119	320	12	0	12	15097.7814
080	7	6	2	14711.3567	221	12	5	7	15997.6941	320	12	1	11	15347.9680
080	7	6	1	14711.3567	221	12	6	7	16073.4901	320	12	3	9	15707.1466
080	7	7	1	15156.0679	221	12	6	6	16077.4540	320	12	5	7	15995.2242
080	7	7	0	15156.0679	221	13	0	13	15342.4286	320	13	1	13	15328.9501
080	8	4	4	13831.1790	221	13	1	12	15615.9489	320	13	2	12	15604.3473
080	8	6	3	14904.6576	221	13	2	11	15844.1991	320	13	2	11	15827.5377
080	8	6	2	14904.6581	221	13	3	11	15842.5247	320	13	3	10	16008.7200
080	8	7	2	15349.8992	221	13	4	10	16030.2053	320	13	4	9	16133.0885
080	9	6	3	15120.5365	221	13	4	9	16138.7978	320	14	0	14	15590.3971
080	10	6	5	15167.5044	221	14	2	13	15886.7765	400	7	6	1	14988.1654
080	10	7	4	15713.4342	221	14	2	12	16132.6648	400	10	7	3	15659.8652
080	13	6	7	16195.4338	221	14	3	12	16132.6633	400	10	9	2	16028.6460
090	2	2	1	13629.2914	221	15	1	15	15854.8955	400	10	9	1	16028.6460
090	8	2	7	14452.4232	231	11	1	11	16359.0810	400	11	5	7	15629.8267
090	11	3	9	14450.3436	240	4	4	0	13932.6666	400	11	5	6	15640.8602
090	13	1	12	15616.7724	240	9	3	6	14591.7595	400	12	2	11	15478.7722 ^c
122	9	2	8	14958.6570	240	9	4	6	14760.8125	400	12	4	8	15893.6774
										400	13	2	12	15727.2790

Notes

^a Term value determined from the 13153.24948 cm⁻¹ line position assigned to the $6\nu_2+\nu_3 6_{52} - 7_{53}$ transition in Ref. [14] but not included in Table 1 of that paper.

^b Term value of this level is new compare to W2020 but corrected compare to its value given in Table 1 of Ref. [14] (14064.39737 cm⁻¹). It was determined from the 13133.15976 cm⁻¹ line position assigned to the $6\nu_2+\nu_3 7_{44} - 7_{43}$ transition in Ref. [14].

^c Term value determined from the 13064.05022 cm⁻¹ line position assigned to the $4\nu_1 12_{211} - 13_{310}$ transition in Ref. [14] but not included in Table 1 of that paper.

Table 2

Energy levels of H₂¹⁶O derived from the analysis of the CRDS spectrum of water vapor in the 13170 – 13418 cm⁻¹ range, showing differences larger than 5×10⁻³ cm⁻¹ with the corresponding W2020 empirical values [19].

V ₁ V ₂ V ₃	J	K _a	K _c	Energy level (cm ⁻¹)			UncW2020 (cm ⁻¹)	R ^g
				This Work	W2020	Difference (TW-W2020)		
023	13	2	12	16043.0830	16042.93989	0.1431	0.02864	5.00
033	6	0	6	15962.8014	15962.80883	-0.0074	0.00132	5.63
042	2	1	2	13546.5924	13546.75517	-0.1628	0.00166	98.05
042	2	2	1	13647.2401	13647.23441	0.0057	0.02527	0.23
042	2	2	0	13648.2180	13648.12927	0.0887	0.01562	5.68
042	3	0	3	13589.1342	13589.14019	-0.0060	0.00124	4.83
042	3	2	1	13722.5190	13722.52663	-0.0076	0.00192	3.97
042	4	1	4	13685.3858	13685.56790	-0.1821	0.00102	178.53
042	4	4	1	14136.5778	14136.80165	-0.2238	0.00607	36.88
042	5	1	5	13782.6735	13782.68636	-0.0129	0.00800	1.61
042	6	2	5	14061.7748	14061.75366	0.0211	0.00800	2.64
042	6	3	3	14228.8163	14229.14990	-0.3336	0.00400	83.40
042	6	5	2	14617.9028	14617.90809	-0.0053	0.00183	2.89
042	7	0	7	14025.9510	14026.30928	-0.3583	0.00176	203.57
042	7	1	6	14193.2848	14193.36940	-0.0846	0.03179	2.66
042	7	3	4	14403.4646	14403.50611	-0.0415	0.00200	2.08
042	7	4	3	14570.4645	14570.46973	-0.0052	0.00437	1.20
042	8	0	8	14178.1135	14178.10163	0.0119	0.01881	0.63
042	9	1	8	14571.2806	14571.30647	-0.0259	0.01306	1.98
042	9	4	5	14982.8945	14982.93032	-0.0358	0.00587	6.10
042	10	4	7	15213.1227	15213.10911	0.0136	0.00400	3.40
042	10	4	6	15262.5683	15262.59529	-0.0270	0.00800	3.37
042	11	0	11	14733.2767	14733.25852	0.0182	0.01331	1.37
052	5	3	2	15554.0671	15554.07294	-0.0058	0.00229	2.55
061	5	4	2	13752.0423	13752.03640	0.0059	0.00400	1.48
061	8	6	2	14900.0058	14900.54575	-0.5400	0.00400	134.99
061	10	2	8	14228.6084	14228.44897	0.1594	0.01150	13.86
061	11	6	6	15749.1539	15749.04110	0.1128	0.00402	28.07
061	11	6	5	15750.3809	15750.99418	-0.6133	0.00501	122.46
080	10	4	6	14273.1320	14273.13841	-0.0064	0.01320	0.49
090	5	2	3	13894.7610	13895.03236	-0.2714	0.00400	67.84
090	8	1	8	13781.4259	13781.48247	-0.0566	0.02033	2.78
090	10	1	10	14203.5563	14203.72439	-0.1681	0.02088	8.05
103	10	2	8	15660.7193	15660.72549	-0.0062	0.00198	3.12
103	10	4	6	15841.0284	15841.04062	-0.0122	0.00108	11.30
122	7	2	6	14611.7662	14611.77179	-0.0056	0.00186	3.01
122	7	3	4	14758.0609	14758.06636	-0.0055	0.00159	3.44
122	8	3	5	14962.4414	14962.45230	-0.0109	0.00159	6.84
122	8	6	3	15402.9281	15402.93569	-0.0076	0.00163	4.67
122	9	0	9	14777.6257	14777.63102	-0.0053	0.01260	0.42
122	9	1	9	14777.0497	14777.07422	-0.0245	0.00603	4.06
122	9	2	7	15102.2205	15102.21512	0.0054	0.00184	2.93
122	9	3	7	15118.9024	15118.84085	0.0616	0.00800	7.69
122	9	4	5	15290.1930	15290.20530	-0.0123	0.01729	0.71
141	0	0	0	13256.1592	13256.15296	0.0062	0.00400	1.56
141	2	1	2	13350.1361	13350.13076	0.0053	0.00147	3.64
141	2	1	1	13369.4092	13369.41533	-0.0061	0.00141	4.34
141	3	1	2	13447.9152	13447.92126	-0.0061	0.00943	0.64
141	3	3	1	13673.9407	13673.94576	-0.0051	0.00235	2.16
141	4	3	2	13769.0324	13769.04027	-0.0079	0.00177	4.45

141	5	5	0	14300.6885	14300.69691	-0.0084	0.00150	5.59
141	8	4	5	14579.5898	14579.58377	0.0060	0.02000	0.30
141	9	5	5	15020.7492	15020.76419	-0.0150	0.00403	3.72
141	9	7	2	15416.5470 ^a	15416.54164	0.0054	0.00810	0.66
141	10	4	6	15034.6811	15034.68925	-0.0081	0.00471	1.73
141	10	7	3	15650.3816 ^b	15650.38727	-0.0057	0.00839	0.68
151	7	3	5	15681.9580	15681.95246	0.0055	0.00399	1.39
160	6	4	2	13836.5522	13836.57303	-0.0208	0.01265	1.65
170	7	1	7	14429.6280	14429.63338	-0.0054	0.00160	3.37
202	11	2	9	15788.9433	15789.21872	-0.2754	0.00800	34.42
202	11	5	6	16088.0896	16088.09592	-0.0063	0.01115	0.57
211	11	5	7	14089.8364	14089.84160	-0.0052	0.00175	2.97
221	5	4	1	14300.6217	14300.61620	0.0055	0.00102	5.37
221	6	5	2	14648.4169 ^c	14648.42249	-0.0056	0.00372	1.50
221	8	2	7	14516.9736	14516.97915	-0.0056	0.00197	2.82
221	9	3	6	14923.3613	14923.36707	-0.0058	0.00420	1.37
221	10	2	8	15074.9955	15075.00261	-0.0071	0.00146	4.88
221	11	1	11	14896.6347	14896.63989	-0.0052	0.00294	1.76
221	11	2	9	15311.1999	15311.19345	0.0065	0.00137	4.71
221	13	1	13	15342.3588	15342.36858	-0.0098	0.01869	0.52
221	13	2	12	15615.1969	15615.49721	-0.3003	0.00402	74.74
221	14	0	14	15576.6425	15576.62632	0.0162	0.01763	0.92
231	4	2	2	15456.3271	15456.33215	-0.0051	0.00103	4.89
231	6	0	6	15543.9860	15543.99215	-0.0061	0.00240	2.56
231	6	1	5	15662.0080	15662.01361	-0.0056	0.00369	1.52
231	6	3	3	15824.0949	15824.10086	-0.0060	0.00124	4.80
231	7	5	2	16304.6115	16304.60398	0.0075	0.00153	4.92
231	8	1	8	15818.6233	15818.63505	-0.0117	0.00587	2.00
231	8	2	7	16002.4459	16002.45373	-0.0078	0.01168	0.67
231	8	3	5	16201.6948	16201.72003	-0.0252	0.00102	24.74
231	8	4	4	16324.6050	16324.62052	-0.0155	0.00169	9.19
231	9	0	9	15984.1090	15984.11976	-0.0108	0.00281	3.83
240	6	2	4	13865.7616	13865.77439	-0.0128	0.02515	0.51
240	6	3	4	13992.9619	13992.95680	0.0051	0.00158	3.23
240	6	4	2	14193.0305	14193.06017	-0.0297	0.00403	7.36
240	6	5	1	14426.6828	14426.58859	0.0942	0.00800	11.78
240	7	2	5	14047.3010	14047.28580	0.0152	0.00400	3.80
240	7	3	4	14166.9010	14166.90935	-0.0084	0.00369	2.27
240	7	4	4	14361.4600	14361.44684	0.0132	0.00620	2.12
240	7	6	2	14850.2936	14850.28613	0.0075	0.01074	0.70
240	7	6	1	14850.2931	14850.28677	0.0063	0.00132	4.79
240	8	4	4	14548.8192	14548.89307	-0.0739	0.00500	14.77
240	8	5	3	14783.2451	14783.25211	-0.0070	0.00125	5.60
240	8	8	1	15405.1000	15405.10694	-0.0069	0.00188	3.70
240	8	8	0	15405.1000	15405.10843	-0.0084	0.00166	5.08
240	9	4	5	14762.9640	14762.97125	-0.0073	0.01320	0.55
240	9	5	5	14995.9539	14995.93699	0.0169	0.00500	3.38
240	9	6	3	15252.8070	15252.82151	-0.0145	0.01030	1.41
240	10	2	8	14720.5750	14720.59751	-0.0225	0.00300	7.50
240	11	4	8	15251.6521	15251.63343	0.0187	0.07730	0.24
240	12	5	7	15781.2620	15781.34935	-0.0874	0.00503	17.35
301	4	1	4	14039.3778	14039.38387	-0.0061	0.00101	5.99
301	4	1	3	14088.3327	14088.32538	0.0073	0.00100	7.31
301	9	8	2	15612.4499 ^d	15612.61816	-0.1683	0.00965	17.44
301	9	8	1	15612.4506 ^e	15612.61668	-0.1661	0.01038	16.00
301	10	1	10	14867.3851	14867.39188	-0.0068	0.00166	4.09
301	10	7	4	15686.0043	15686.01092	-0.0066	0.01410	0.47
301	10	8	3	15840.7658	15840.79950	-0.0337	0.00802	4.20

301	10	8	2	15840.7247	15840.73035	-0.0057	0.00194	2.92
301	11	6	6	15795.0549	15795.00555	0.0494	0.00193	25.56
301	11	7	5	15905.3247	15904.86217	0.4625	0.01840	25.14
301	12	2	10	15657.7881	15657.79587	-0.0078	0.00656	1.19
301	12	3	10	15658.5351	15658.54082	-0.0057	0.00199	2.87
301	12	3	9	15814.9370	15814.94336	-0.0064	0.00710	0.90
301	12	4	9	15817.3848	15817.37733	0.0075	0.00300	2.49
301	13	1	12	15730.2969	15730.30219	-0.0053	0.00031	16.80
301	14	0	14	15759.0498	15759.06149	-0.0117	0.00453	2.58
301	14	1	14	15759.1277	15759.13615	-0.0085	0.00491	1.72
301	14	1	13	15996.4584	15996.46582	-0.0074	0.01053	0.70
301	15	0	15	16023.8212	16023.73457	0.0866	0.02019	4.29
301	15	1	15	16023.7618	16023.77023	-0.0084	0.00101	8.38
301	15	2	14	16276.2951	16276.28945	0.0057	0.02233	0.25
301	16	0	16	16305.1447	16305.12988	0.0148	0.00622	2.38
320	7	1	7	14196.5329	14196.53840	-0.0055	0.00109	5.06
320	7	4	4	14598.0564	14598.06262	-0.0062	0.00135	4.61
320	8	2	7	14505.8284	14505.83580	-0.0074	0.00550	1.34
320	8	7	2	15265.2187	15265.20843	0.0103	0.00189	5.45
320	8	7	1	15265.2191	15265.20835	0.0108	0.00180	5.97
320	9	4	5	15009.6072	15009.61555	-0.0083	0.00800	1.04
320	9	7	3	15477.8881	15477.91500	-0.0269	0.00150	17.93
320	9	7	2	15477.8874	15477.92119	-0.0338	0.01055	3.20
320	10	2	8	15061.2370	15061.22927	0.0077	0.00530	1.46
320	10	5	6	15441.6903	15441.70466	-0.0144	0.01086	1.32
320	11	0	11	14884.1511	14884.15833	-0.0072	0.01161	0.62
320	11	3	8	15424.8515	15424.86281	-0.0113	0.00400	2.83
320	12	1	12	15098.0372	15098.12389	-0.0867	0.01241	6.99
320	13	1	12	15603.7950	15603.80171	-0.0067	0.00800	0.84
330	7	2	6	15824.2795	15824.29200	-0.0125	0.00193	6.46
400	4	2	3	14104.8948	14104.90075	-0.0060	0.00102	5.81
400	5	0	5	14131.1261	14131.13571	-0.0096	0.00165	5.81
400	6	6	1	14747.6048	14747.61363	-0.0088	0.00293	3.01
400	6	6	0	14747.6170	14747.61141	0.0056	0.00248	2.25
400	7	5	2	14809.7429	14809.74816	-0.0053	0.00128	4.11
400	7	6	2	14988.1490	14988.04615	0.1028	0.00800	12.86
400	8	2	6	14745.1983	14745.20503	-0.0067	0.00259	2.60
400	8	3	5	14809.2336	14809.23903	-0.0054	0.00115	4.72
400	8	6	3	15178.8380	15178.82996	0.0080	0.00300	2.68
400	9	1	9	14683.8670	14683.87381	-0.0068	0.00179	3.80
400	9	6	4	15304.9733	15304.95952	0.0138	0.00925	1.49
400	9	6	3	15305.4608	15305.47574	-0.0149	0.00220	6.80
400	9	7	3	15432.7669	15432.68450	0.0824	0.00100	82.40
400	10	1	9	15031.0451	15031.05605	-0.0110	0.00121	9.08
400	10	6	4	15539.5462	15539.20909	0.3371	0.00800	42.14
400	11	3	9	15403.7522	15403.75939	-0.0072	0.00800	0.90
400	11	3	8	15551.7330	15551.74248	-0.0095	0.00307	3.09
400	11	4	8	15548.0785	15548.00703	0.0715	0.00430	16.61
400	11	6	6	15792.1287	15792.11710	0.0116	0.00300	3.87
400	12	2	10	15652.8164	15652.82282	-0.0064	0.00800	0.80
400	12	3	9	15797.1568	15797.14826	0.0085	0.00718	1.19

Notes

^a The W2020 $V_1V_2V_3JK_aK_c$ assignment is 061 9 7 2

^b The W2020 assignment is 061 10 7 3

^c The W2020 assignment is 301 6 5 2

^d The W2020 assignment is 221 9 8 2

^e The W2020 assignment is 221 9 8 1

${}^s R = \frac{|TW - W_{2020}|}{UncW_{2020}}$ is the ratio of the absolute deviation of the W2020 energy level value from the value derived from the present CRDS recordings by the corresponding W2020 uncertainty [19].

References

1. Mikhailenko S, Kassi S, Mondelain D, Campargue A. Water vapor absorption between 5690 and 8340 cm^{-1} : accurate empirical line centers and validation tests of calculated line intensities. *J Quant Spectrosc Radiat Transf* 2020;245:106840. doi: [10.1016/j.jqsrt.2020.106840](https://doi.org/10.1016/j.jqsrt.2020.106840)
2. Mikhailenko SN, Kassi S, Mondelain D, Gamache RR, Campargue A. A spectroscopic database for water vapor between 5850 and 8340 cm^{-1} . *J Quant Spectrosc Radiat Transf* 2016;179:198–216. doi: doi.org/10.1016/j.jqsrt.2016.03.035
3. Sironneau VT, Hodges JT. Line shapes, positions and intensities of water transitions near 1.28 μm . *J Quant Spectrosc Radiat Transf* 2015;152:1–15. doi: doi.org/10.1016/j.jqsrt.2014.10.020
4. Coheur PF, Fally S, Carleer M, Clerbaux C, Colin R, Jenouvrier A, et al. New water vapor line parameters in the 26000 – 13000 cm^{-1} region. *J Quant Spectrosc Radiat Transf* 2002;74:493–510. [https://doi.org/10.1016/S0022-4073\(01\)00269-2](https://doi.org/10.1016/S0022-4073(01)00269-2)
5. Mérienne MF, Jenouvrier A, Hermans C, Vandaele AC, Carleer M, Clerbaux C, et al. Water vapor line parameters in the 13 000 9250 cm^{-1} region. *J Quant Spectrosc Radiat Transf* 2003;82:99–117. [https://doi.org/10.1016/S0022-4073\(03\)00148-1](https://doi.org/10.1016/S0022-4073(03)00148-1)
6. Schermaul R, Learner RCM, Newnham DA, Ballard J, Zobov NF, Belmiloud D, et al. The water vapor spectrum in the region 8600–15 000 cm^{-1} : Experimental and theoretical studies for a new spectral line database: I. Laboratory measurements *J Mol Spectrosc* 2001;208:32–42. doi: doi.org/10.1006/jmsp.2001.8373
7. Schermaul R, Learner RCM, Newnham DA, Ballard J, Zobov NF, Belmiloud D, et al. The water vapor spectrum in the region 8600 – 15 000 cm^{-1} : Experimental and theoretical studies for a new spectral line database: II. Linelist construction. *J Mol Spectrosc* 2001;208:43–50. <https://doi.org/10.1006/jmsp.2001.8374>
8. Tolchenov RN, Naumenko O, Zobov NF, Shirin SV, Polyansky OL, Tennyson J, et al. Water vapour line assignments in the 9250 – 26 000 cm^{-1} frequency range. *J Mol Spectrosc* 2005;233:68–76. <https://doi.org/10.1016/j.jms.2005.05.015>
9. Tolchenov RN, Tennyson J, Brault JW, Canas AAD, Schermaul R. Weak line water vapor spectrum in the 11 787 – 13 554 cm^{-1} region. *J Mol Spectrosc* 2002;215:269–74. <https://doi.org/10.1006/jmsp.2002.8653>
10. Tolchenov RN, Tennyson J. Water line parameters from refitted spectra constrained by empirical upper state levels: study of the 9500 – 14500 cm^{-1} region. *J Quant Spectrosc Radiat Transf* 2008;109:559–68. <https://doi.org/10.1016/j.jqsrt.2007.08.001>
11. Campargue A, Mikhailenko S, Liu AW. ICLAS of water in the 770 nm transparency window (12 746 – 13 558 cm^{-1}). Comparison with current experimental and calculated databases. *J Quant Spectrosc Radiat Transf* 2008;109:2832–45. doi: doi.org/10.1016/j.jqsrt.2008.07.003
12. Béguier S, Mikhailenko S, Campargue A. The absorption spectrum of water between 13540 and 14070 cm^{-1} : ICLAS detection of weak lines and a complete linelist. *J Mol Spectrosc* 2011;265:106–9. <https://doi.org/10.1016/j.jms.2010.12.002>
13. Kassi S, Macko P, Naumenko O, Campargue A. The absorption spectrum of water near 750 nm by CW-CRDS: contribution to the search of water dimer absorption. *Phys Chem Chem Phys* 2005;7:2460–7. <https://doi.org/10.1039/B502172C>
14. Vasilchenko S, Mikhailenko SN, Campargue A. Water vapor absorption in the region of the oxygen A-band near 760 nm. *J Quant Spectrosc Radiat Transf* 2021;275:107847. doi: doi.org/10.1016/j.jqsrt.2021.107847
15. Gordon IE, Rothman LS, Hargreaves RJ, Hashemi R, Karlovets EV, Skinner FM, et al. The HITRAN2020 molecular spectroscopic database. *J Quant Spectrosc Radiat Transf* 2022;277:107949. <https://doi.org/10.1016/j.jqsrt.2021.107949>
16. Vasilchenko SS, Kassi S, Lugovskoi AA. High-sensitivity cavity ring-down spectrometer for high-resolution spectroscopy of atmospheric gases in the 745–775-nm region. *Atmos Ocean*

- Opt 2021;34:274-7. <https://doi.org/10.1134/S1024856021030179>
17. Pfeilsticker K, Lotter A, Peters C, Bösch H. Atmospheric detection of water dimers via near-infrared absorption. *Science* 2003;300:2078–80. DOI: [10.1126/science.1082282](https://doi.org/10.1126/science.1082282)
 18. Lotter A. PhD thesis. Heidelberg University; 2006. 156 P.
 19. Furtenbacher T, Tóbiás R, Tennyson J, Polyansky OL, Kyuberis AA, Ovsyannikov RI, et al. The W2020 Database of Validated Rovibrational Experimental Transitions and Empirical Energy Levels of Water Isotopologues. II. H₂¹⁷O and H₂¹⁸O with an update to H₂¹⁶O. *J Phys Chem Ref Data* 2020;49:43103. <https://doi.org/10.1063/5.0030680>
 20. Partridge H, Schwenke DW. The determination of an accurate isotope dependent potential energy surface for water from extensive ab initio calculations and experimental data. *J Chem Phys* 1997;106:4618–39. <https://doi.org/10.1063/1.473987>
 21. Schwenke DW, Partridge H. Convergence testing of the analytic representation of an *ab initio* dipole moment function for water: Improved fitting yields improved intensities. *J Chem Phys* 2000;113:6592–7. <https://doi.org/10.1063/1.1311392>
 22. Tashkun SA. Institute of Atmospheric Optics SB RAS. 2007. <http://spectra.iao.ru/molecules/simlaunch?mol=1>
 23. Macko P, Romanini D, Mikhailenko SN, Naumenko OV, Kassi S, Jenouvrier A, et al. High sensitivity CW-cavity ring down spectroscopy of water in the region of the 1.5 μm atmospheric window. *J Mol Spectrosc* 2004;227:90–108. <https://doi.org/10.1016/j.jms.2004.05.020>
 24. Kassi S, Campargue A. Cavity ring down spectroscopy with 5×10⁻¹³ cm⁻¹ sensitivity. *J Chem Phys* 2012;137. <https://doi.org/10.1063/1.4769974>
 25. Grossmann BE, Browell EV. Spectroscopy of water vapor in the 720-nm wavelength region: line strengths, self-induced pressure broadenings and shifts, and temperature dependence of line widths and shifts. *J Mol Spectrosc* 1989;136:264–94. [https://doi.org/10.1016/0022-2852\(89\)90336-6](https://doi.org/10.1016/0022-2852(89)90336-6)
 26. Tennyson J, Bernath PF, Brown LR, Campargue A, Carleer MR, Császár AG, et al. IUPAC critical evaluation of the rotational-vibrational spectra of water vapor. part I energy levels and transition wavenumbers for H₂¹⁷O and H₂¹⁸O. *J Quant Spectrosc Radiat Transf* 2009;110:573–96. doi: doi.org/10.1016/j.jqsrt.2009.02.014
 27. Tennyson J, Bernath PF, Brown LR, Campargue A, Császár AG, Daumont L, et al. IUPAC critical evaluation of the rotational-vibrational spectra of water vapor. Part II. Energy levels and transition wavenumbers for HD¹⁶O, HD¹⁷O, and HD¹⁸O. *J Quant Spectrosc Radiat Transf* 2010;111:2160–84. doi: doi.org/10.1016/j.jqsrt.2010.06.012
 28. Tennyson J, Bernath PF, Brown LR, Campargue A, Császár AG, Daumont L, et al. IUPAC critical evaluation of the rotational-vibrational spectra of water vapor. Part III: energy levels and transition wavenumbers for H₂¹⁶O. *J Quant Spectrosc Radiat Transf* 2013;117:29–58. doi: doi.org/10.1016/j.jqsrt.2012.10.002
 29. Leshchishina OM, Naumenko OV, Campargue A. High sensitivity ICLAS of H₂¹⁸O in the 12580 – 13550 cm⁻¹ transparency window. *J Quant Spectrosc Radiat Transf* 2011;112:913-24. <https://doi.org/10.1016/j.jqsrt.2010.11.012>
 30. Naumenko O, Campargue A, Bertseva E, Schwenke D. Experimental and *ab initio* studies of the HDO absorption spectrum in the 13165 – 13500 cm⁻¹ spectral region. *J Mol Spectrosc* 2000;201:297-309. <https://doi.org/10.1006/jmsp.2000.8087>
 31. Voronin BA, Naumenko OV, Carleer M, Coheur P-F, Fally S, Jenouvrier A, et al. HDO absorption spectrum above 11 500 cm⁻¹: Assignment and dynamics. *J Mol Spectrosc* 2007;244:87-101. <https://doi.org/10.1016/j.jms.2007.03.008>
 32. Naumenko OV, Béguier S, Leshchishina OM, Campargue A. ICLAS of HDO between 13,020 and 14,115 cm⁻¹. *J Quant Spectrosc Radiat Transf* 2010;111:36-44. <https://doi.org/10.1016/j.jqsrt.2009.06.016>

33. Furtenbacher T, Tobias R, Tennyson J, Polyansky OL, Császár AG. W2020: A database of validated rovibrational experimental transitions and empirical energy levels for H₂¹⁶O. *J Phys Chem Ref Data* 2020;49:033101. doi: doi.org/10.1063/5.0008253
34. Campargue A, Mikhailenko SN, Kassi S, Vasilchenko S. Validation tests of the W2020 energy levels of water vapor. *J Quant Spectrosc Radiat Transf* 2021;276:107914. doi: doi.org/10.1016/j.jqsrt.2021.107914
35. Bubukina II, Zobov NF, Polyansky OL, Shirin SV, Yurchenko SN. Optimized semiempirical potential energy surface for H₂¹⁶O up to 26000 cm⁻¹. *Optics and Spectroscopy* 2011;110:160-166. <https://doi.org/10.1134/S0030400X11020032>
36. Polyansky OL, Kyuberis AA, Zobov NF, Tennyson J, Yurchenko SN, Lodi L. ExoMol molecular line lists XXX: A complete high-accuracy line list for water. *Mon Not R Astron Soc* 2018;480:1–12. <https://doi.org/10.1093/mnras/sty1877>
37. Conway EK, Gordon IE, Kyuberis AA, Polyansky OL, Tennyson J, Zobov NF. Calculated line lists for H₂¹⁶O and H₂¹⁸O with extensive comparisons to theoretical and experimental sources including the HITRAN2016 database. *J Quant Spectrosc Radiat Transf* 2020;241:106711. doi: doi.org/10.1016/j.jqsrt.2019.106711